Supporting Information for "Capability of TEC correlation analysis and deceleration at propagation velocities of MSTID: Preseismic ionospheric anomalies before the large earthquakes"

Ken Umeno[1], Ryo Nakabayashi[1], Takuya Iwata[1], Minghui Kao[1]

[1] Department of Applied Mathematics and Physics, Graduate School of Informatics, Kyoto University, Kyoto, Japan

Contents of this file

1. Figures S1 to S29
2. Table S1

Additional Supporting Information (Files uploaded separately)

1. Captions for Movies S1 and S2

Introduction

Supplementary materials are composed of twenty nine Figures, two Movies, and one Table that help readers understand the manuscript better.

Figure S1 shows the locations of the fifteen GNSS stations used for TEC CoRelation Analysis (CRA) on April 13, 2021 and April 15, 2021 (the day of main shock of the 2016 Kumamoto earthquake).

Figure S2 and Figure S3 show the correlation values at all the GNSS stations in Japan before the 2016 Kumamoto earthquake on 2016/04/15 (UTC) and on 2016/0413 (UTC), respectively.

Figures S4 to S16 show the correlation values for each different central station before the 2016 Kumamoto earthquake April 15, 2016 (UTC).

Figures S17 to S29 show the correlation values for each different central station on April 13, 2016 (UTC).

Movie S1 and Movie S2 show the temporal behavior of $C(T)$ on 2016/0415 (UTC) and on 2016/04/13(UTC), respectively.

Table S1 shows the list of the half periods of MSTID on April 13, 2016 estimated by CRA.

Caption for Movie S1 Movie S1. Correlation values at all the GNSS stations in Japan before the 2016 Kumamoto earthquake during the time range of 14:00-17:00 (UTC) on 2016/04/15. We used every GNSS station as a central station and mapped the results into the Japan map. The GPS satellite PRN 17 is used here. The black x marks represents the epicenter. The earthquake occurrence time is 16:25 UTC on April 15, 2016.

Caption for Movie S2 Movie S2. Correlation values at all the GNSS stations in Japan before the 2016 Kumamoto earthquake during the time range of 14:00-17:00 (UTC) on 2016/04/13. We used every GNSS station as a central station and mapped the results into the Japan map. The GPS satellite PRN 17 is used here.

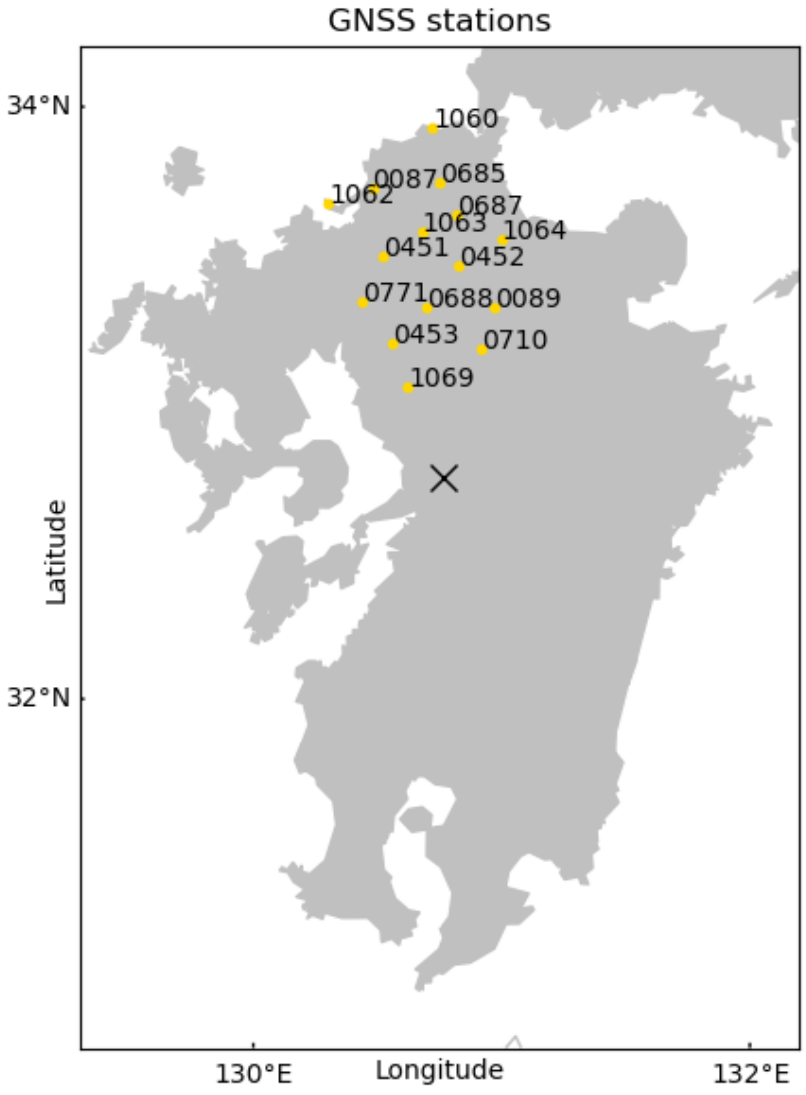

Figure S1. Location of the 15 selected GNSS stations for CRA

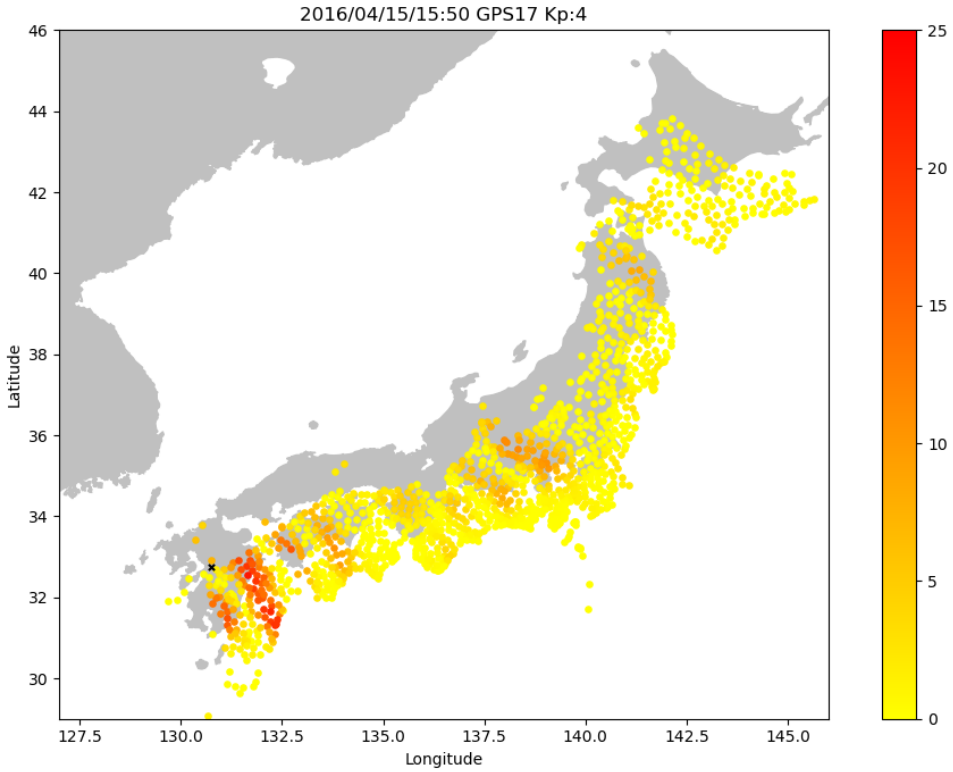

Figure S2. Correlation values at all the GNSS stations in Japan before the 2016 Kumamoto earthquake on 2016/04/15

We used every GNSS station as a central station and mapped the results into the Japan map. The GPS satellite PRN 17 is used here. The black x marks represents the epicenter. The earthquake occurrence time is 16:25 UTC on April 15, 2016 and the time 15:50 in the figure corresponds to 35 minutes before the main shock.

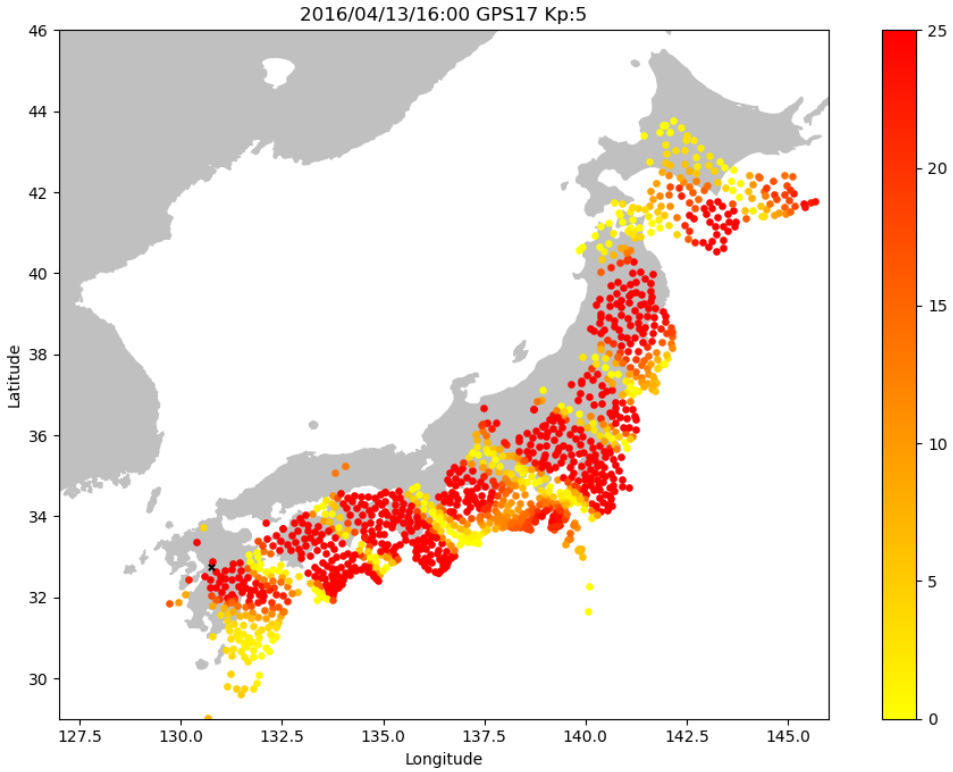

Figure S3. Correlation values at all the GNSS stations in Japan at 16:00 (UTC) on 2016/04/13. No earthquakes occurred on the day while MSTID was observed. We used every GNSS station as a central station and mapped the results onto the Japan map. The GPS satellite RRN17 is used here.

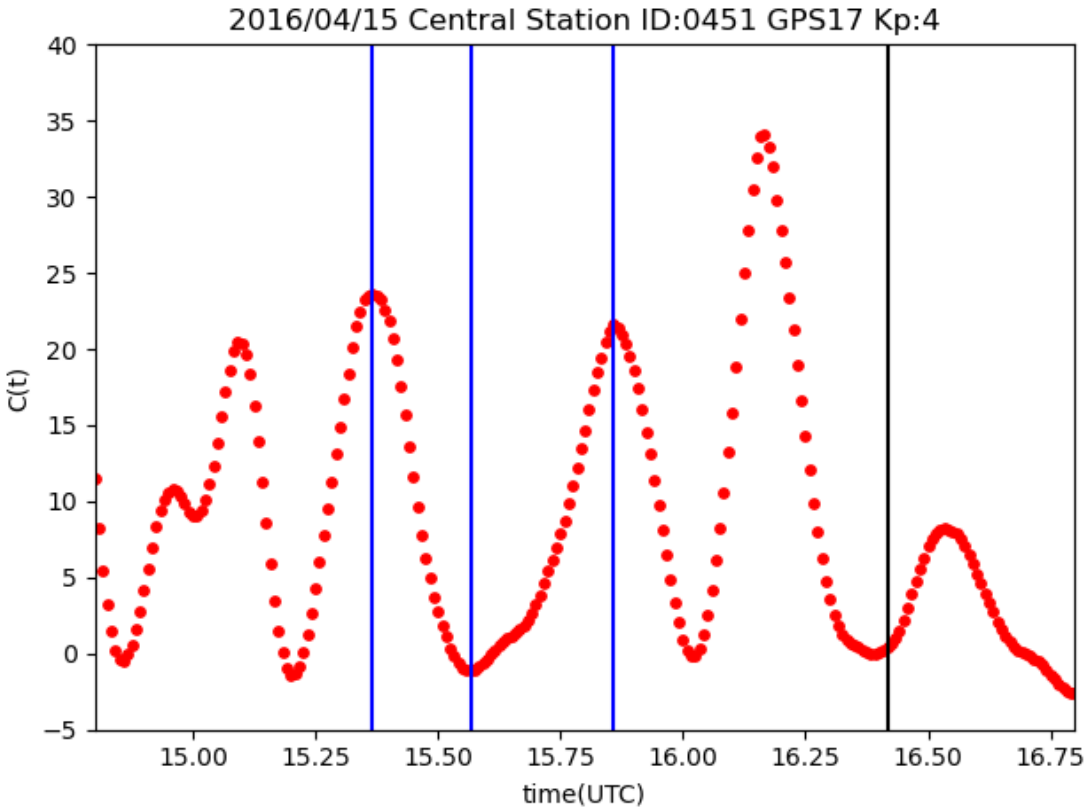

Figure S4. Correlation values before the 2016 Kumamoto earthquake (0451) on April 15, 2016 The vertical axis shows the correlation $C(T)$ and the horizontal one the time t (UTC). The black line indicates the exact time 16:25 (UTC) when the 2016 Kumamoto earthquake occurred. The blue lines indicate the times $t_1, t_2, t_3,\ (t_1 < t_2 < t_3)$ when $C(T)$ has extremal values. Because $0 < \Delta T_1 \equiv t_2 - t_1 < \Delta T_2 \equiv t_3 - t_2$, a deceleration at propagation velocity of MSTID is clarified. The GNSS station 0451 is used as the central station and the GPS satellite RRN17 is selected for the analysis.

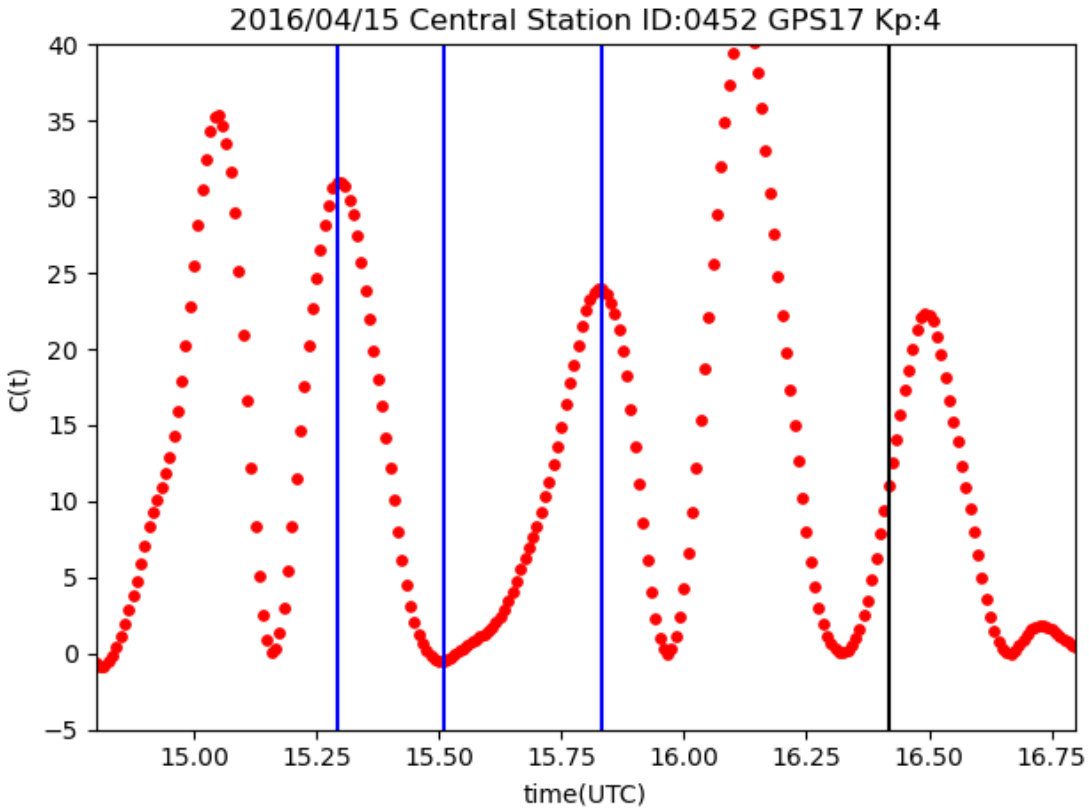

Figure S5. Correlation values before the 2016 Kumamoto earthquake (0452) on April 15, 2016 The vertical axis shows the correlation $C(T)$ and the horizontal one the time t (UTC). The black line indicates the exact time 16:25 (UTC) when the 2016 Kumamoto earthquake occurred. The blue lines indicate the times $t_1, t_2, t_3,\ (t_1 < t_2 < t_3)$ when $C(T)$ has extremal values. Because $0 < \Delta T_1 \equiv t_2 - t_1 < \Delta T_2 \equiv t_3 - t_2$, a deceleration at propagation velocity of MSTID is clarified. The GNSS station 0452 is used as the central station and the GPS satellite RRN17 is selected for the analysis.

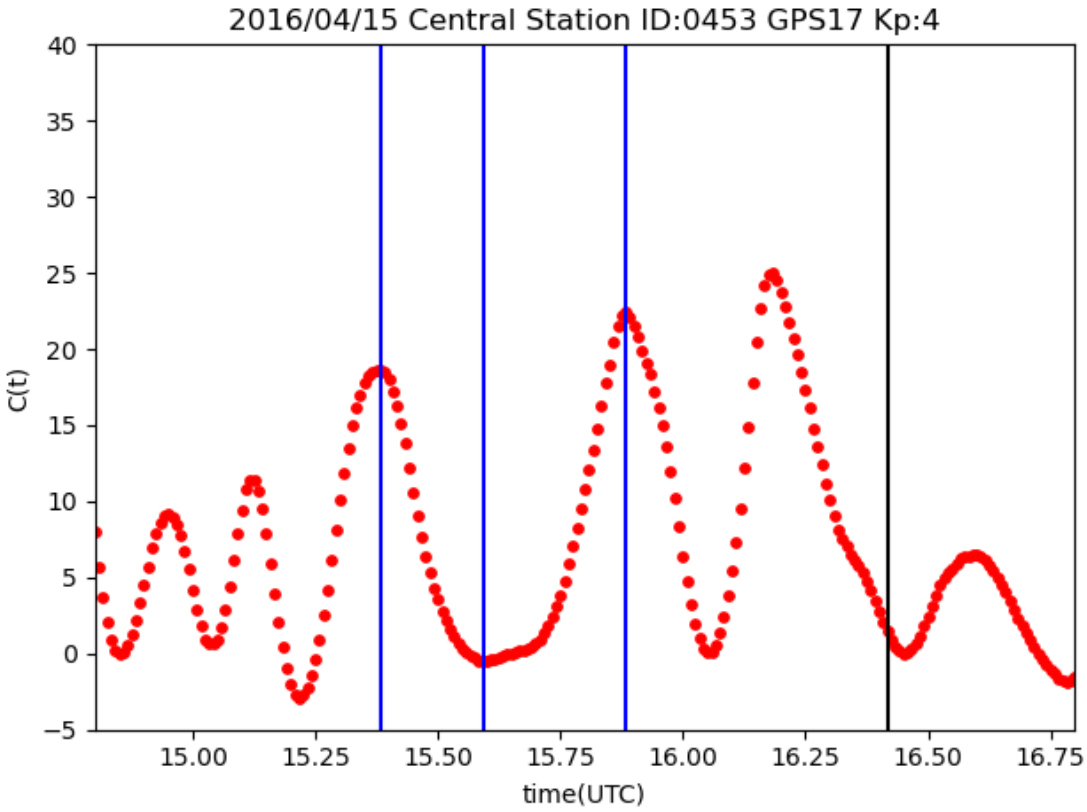

Figure S6. Correlation values before the 2016 Kumamoto earthquake (0453) on April 15, 2016 The vertical axis shows the correlation $C(T)$ and the horizontal one the time t (UTC). The black line indicates the exact time 16:25 (UTC) when the 2016 Kumamoto earthquake occurred. The blue lines indicate the times $t_1, t_2, t_3,\ (t_1 < t_2 < t_3)$ when $C(T)$ has extremal values. Because $0 < \Delta T_1 \equiv t_2 - t_1 < \Delta T_2 \equiv t_3 - t_2$, a deceleration at propagation velocity of MSTID is clarified. The GNSS station 0453 is used as the central station and the GPS satellite RRN17 is selected for the analysis.

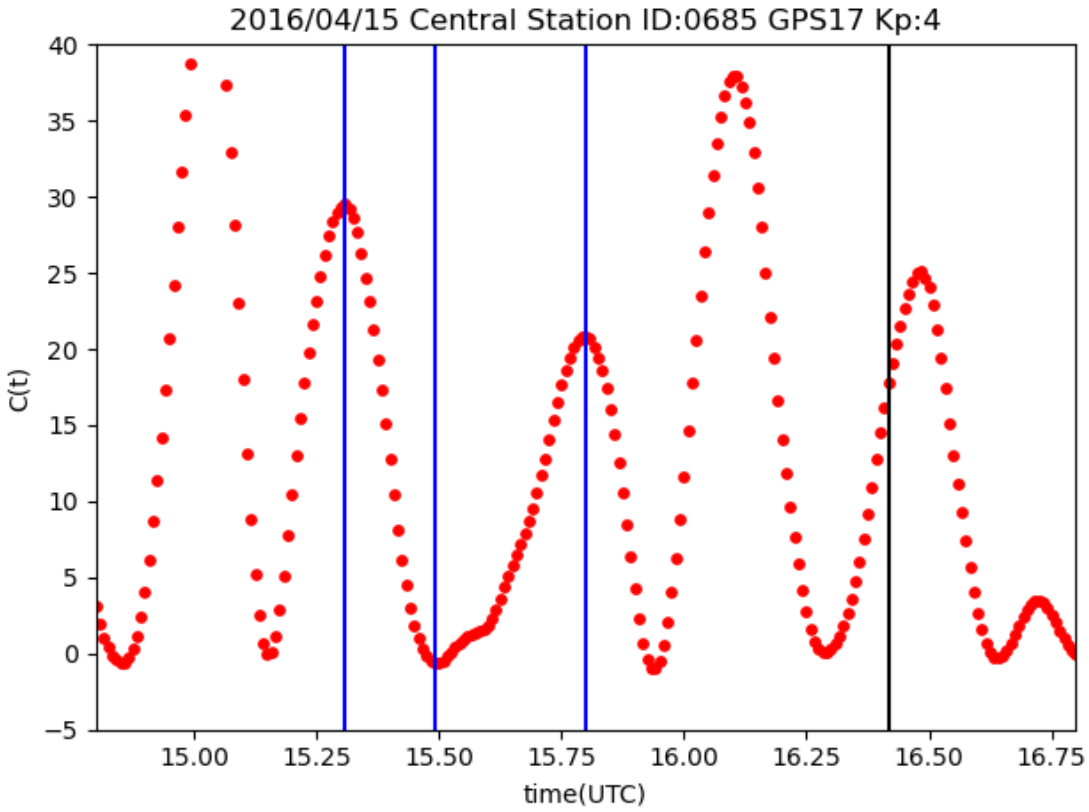

Figure S7. Correlation values before the 2016 Kumamoto earthquake (0685) on April 15, 2016 The vertical axis shows the correlation $C(T)$ and the horizontal one the time t (UTC). The black line indicates the exact time 16:25 (UTC) when the 2016 Kumamoto earthquake occurred. The blue lines indicate the times $t_1, t_2, t_3,\ (t_1 < t_2 < t_3)$ when $C(T)$ has extremal values. Because $0 < \Delta T_1 \equiv t_2 - t_1 < \Delta T_2 \equiv t_3 - t_2$, a deceleration at propagation velocity of MSTID is clarified. The GNSS station 0685 is used as the central station and the GPS satellite RRN17 is selected for the analysis.

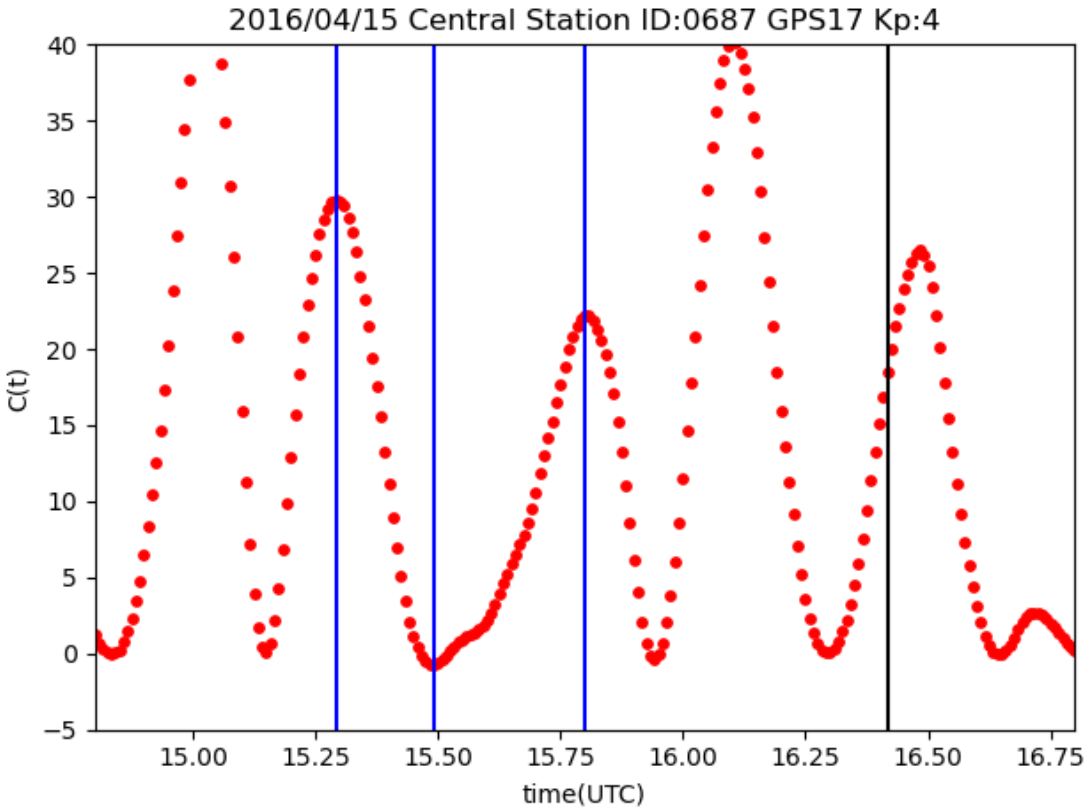

Figure S8. Correlation values before the 2016 Kumamoto earthquake (0687) on April 15, 2016 The vertical axis shows the correlation $C(T)$ and the horizontal one the time t (UTC). The black line indicates the exact time 16:25 (UTC) when the 2016 Kumamoto earthquake occurred. The blue lines indicate the times $t_1, t_2, t_3,\ (t_1 < t_2 < t_3)$ when $C(T)$ has extremal values. Because $0 < \Delta T_1 \equiv t_2 - t_1 < \Delta T_2 \equiv t_3 - t_2$, a deceleration at propagation velocity of MSTID is clarified. The GNSS station 0687 is used as the central station and the GPS satellite RRN17 is selected for the analysis.

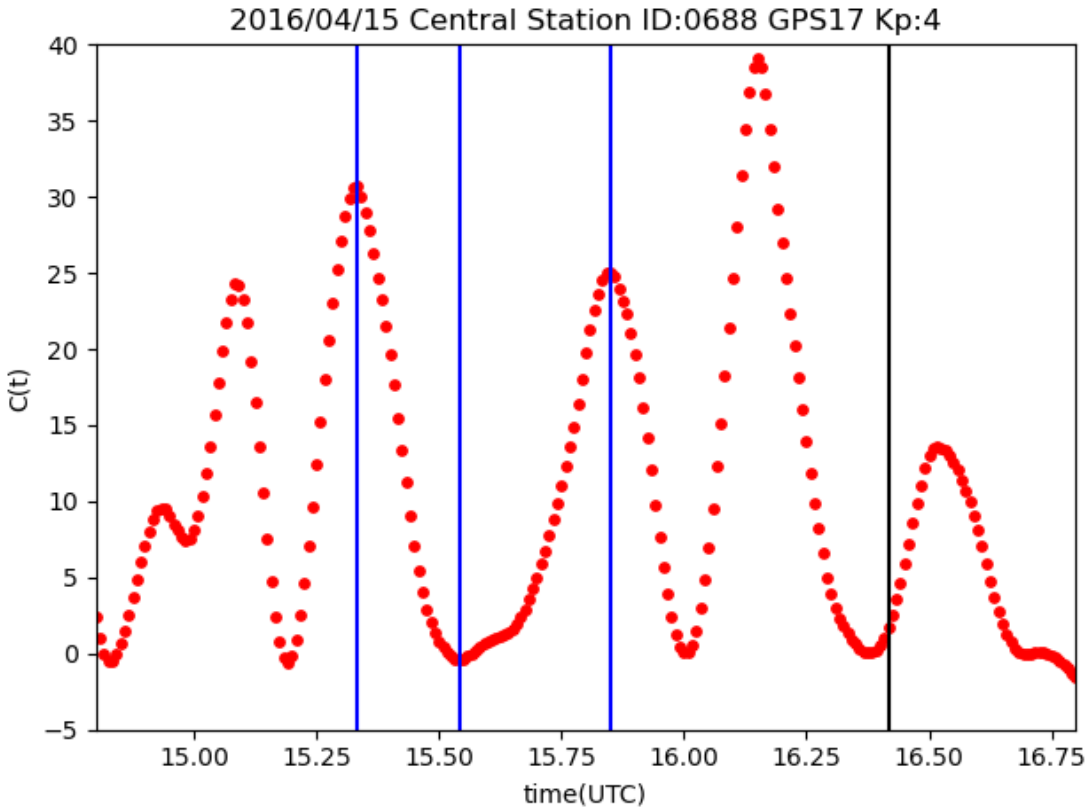

Figure S9. Correlation values before the 2016 Kumamoto earthquake (0688) on April 15, 2016 The vertical axis shows the correlation $C(T)$ and the horizontal one the time t (UTC). The black line indicates the exact time 16:25 (UTC) when the 2016 Kumamoto earthquake occurred. The blue lines indicate the times $t_1, t_2, t_3,\ (t_1 < t_2 < t_3)$ when $C(T)$ has extremal values. Because $0 < \Delta T_1 \equiv t_2 - t_1 < \Delta T_2 \equiv t_3 - t_2$, a deceleration at propagation velocity of MSTID is clarified. The GNSS station 0688 is used as the central station and the GPS satellite RRN17 is selected for the analysis.

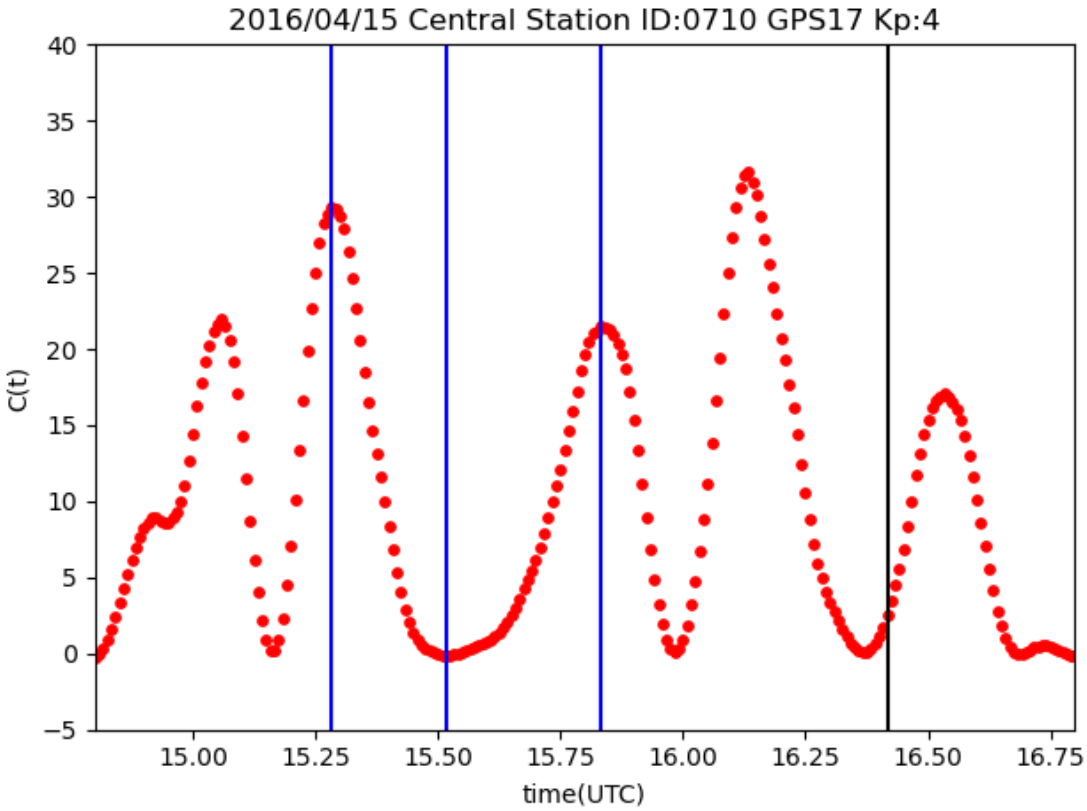

Figure S10. Correlation values before the 2016 Kumamoto earthquake (0710) on April 15, 2016

The vertical axis shows the correlation $C(T)$ and the horizontal one the time t (UTC). The black line indicates the exact time 16:25 (UTC) when the 2016 Kumamoto earthquake occurred. The blue lines indicate the times $t_1, t_2, t_3,\ (t_1 < t_2 < t_3)$ when $C(T)$ has extremal values. Because $0 < \Delta T_1 \equiv t_2 - t_1 < \Delta T_2 \equiv t_3 - t_2$, a deceleration at propagation velocity of MSTID is clarified. The GNSS station 0710 is used as the central station and the GPS satellite RRN17 is selected for the analysis.

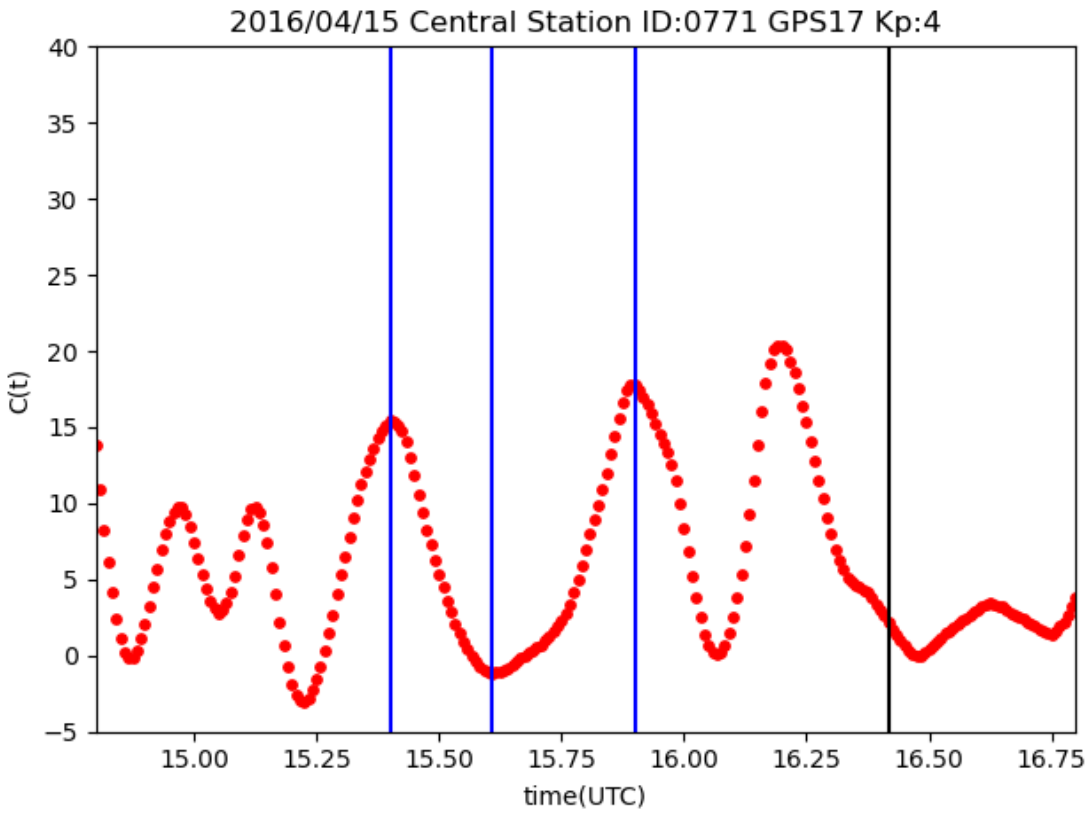

Figure S11. Correlation values before the 2016 Kumamoto earthquake (0711) on April 15, 2016

The vertical axis shows the correlation $C(T)$ and the horizontal one the time t (UTC). The black line indicates the exact time 16:25 (UTC) when the 2016 Kumamoto earthquake occurred. The blue lines indicate the times $t_1, t_2, t_3,\ (t_1 < t_2 < t_3)$ when $C(T)$ has extremal values. Because $0 < \Delta T_1 \equiv t_2 - t_1 < \Delta T_2 \equiv t_3 - t_2$, a deceleration at propagation velocity of MSTID is clarified. The GNSS station 0711 is used as the central station and the GPS satellite RRN17 is selected for the analysis.

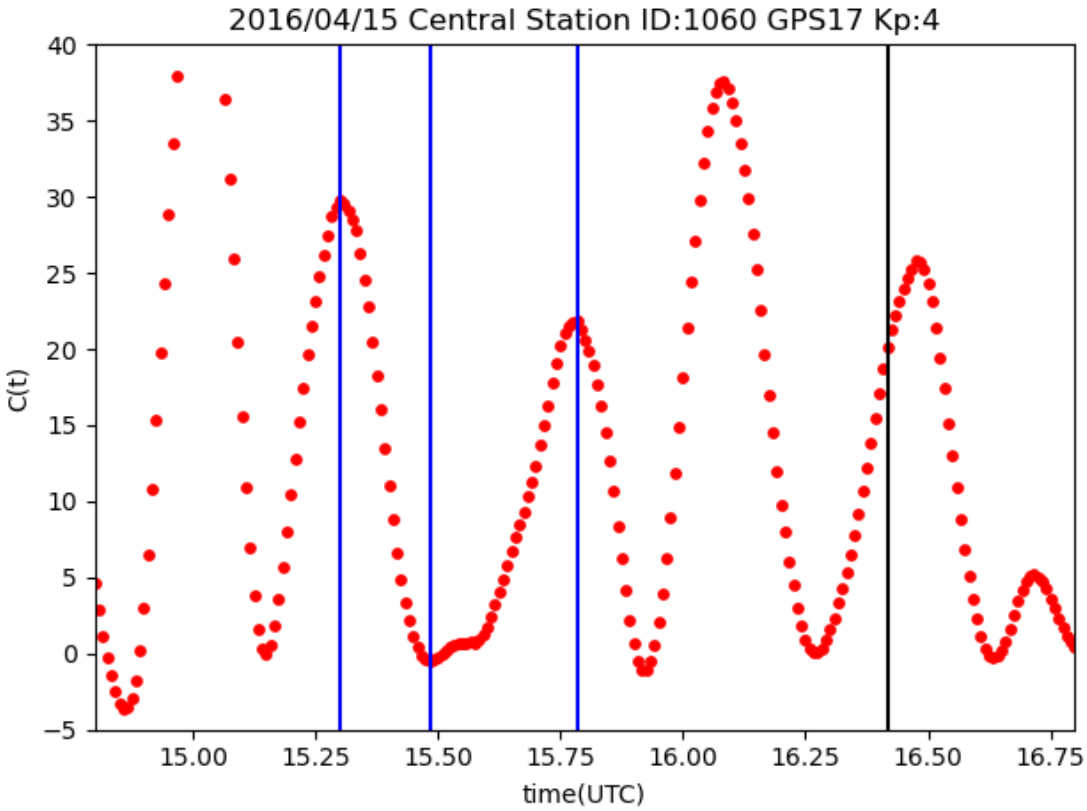

Figure S12. Correlation values before the 2016 Kumamoto earthquake (1060) on April 15, 2016

The vertical axis shows the correlation $C(T)$ and the horizontal one the time t (UTC). The black line indicates the exact time 16:25 (UTC) when the 2016 Kumamoto earthquake occurred. The blue lines indicate the times $t_1, t_2, t_3,\ (t_1 < t_2 < t_3)$ when $C(T)$ has extremal values. Because $0 < \Delta T_1 \equiv t_2 - t_1 < \Delta T_2 \equiv t_3 - t_2$, a deceleration at propagation velocity of MSTID is clarified. The GNSS station 1060 is used as the central station and the GPS satellite RRN17 is selected for the analysis.

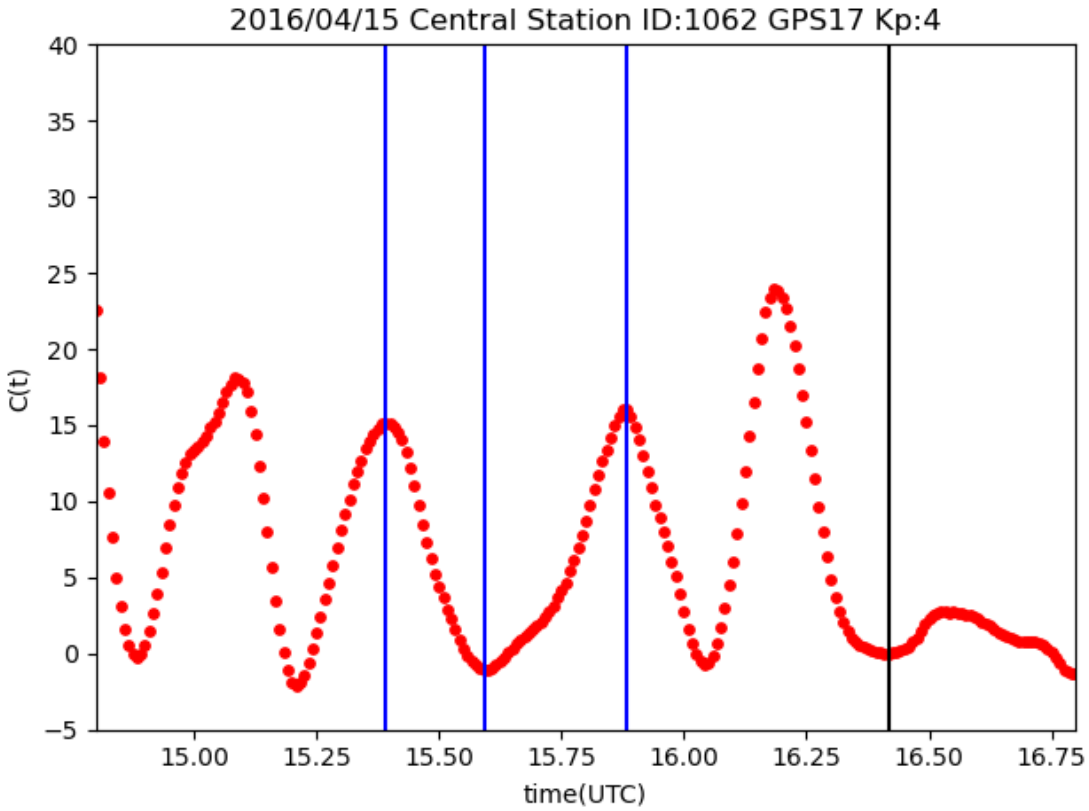

Figure S13. Correlation values before the 2016 Kumamoto earthquake (1062) on April 15, 2016

The vertical axis shows the correlation $C(T)$ and the horizontal one the time t (UTC). The black line indicates the exact time 16:25 (UTC) when the 2016 Kumamoto earthquake occurred. The blue lines indicate the times $t_1, t_2, t_3,\ (t_1 < t_2 < t_3)$ when $C(T)$ has extremal values. Because $0 < \Delta T_1 \equiv t_2 - t_1 < \Delta T_2 \equiv t_3 - t_2$, a deceleration at propagation velocity of MSTID is clarified. The GNSS station 1062 is used as the central station and the GPS satellite RRN17 is selected for the analysis.

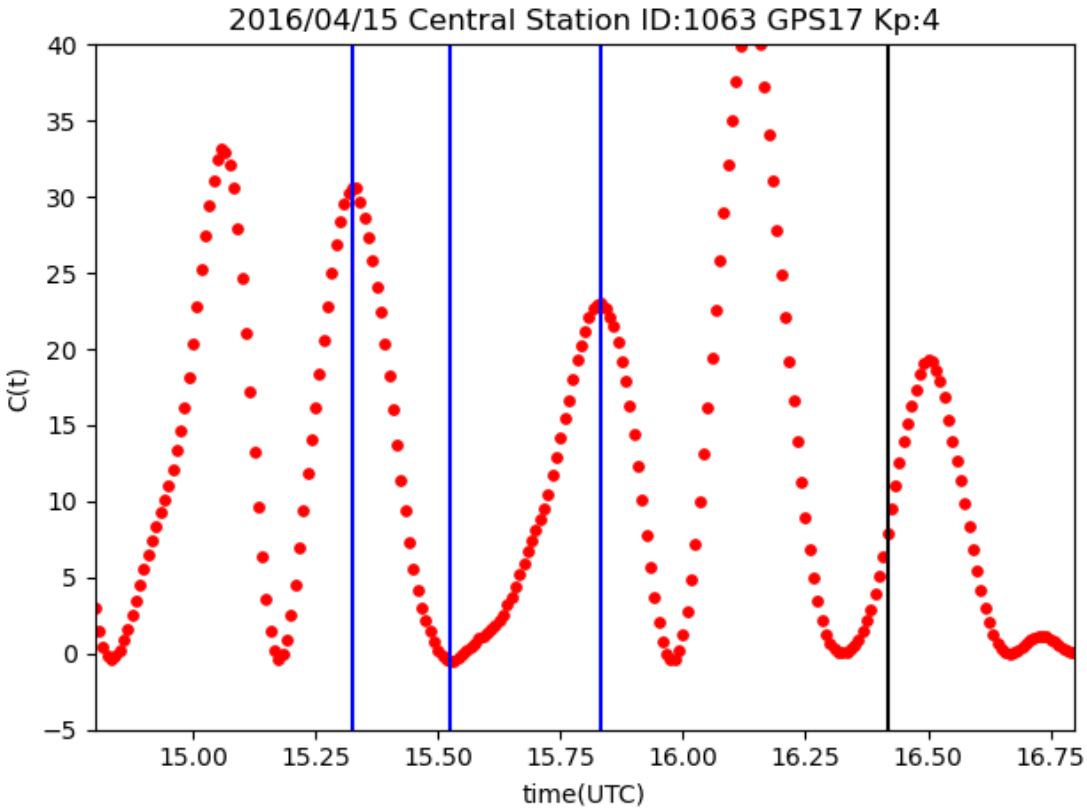

Figure S14. Correlation values before the 2016 Kumamoto earthquake (1063) on April 15, 2016

The vertical axis shows the correlation $C(T)$ and the horizontal one the time t (UTC). The black line indicates the exact time 16:25 (UTC) when the 2016 Kumamoto earthquake occurred. The blue lines indicate the times $t_1, t_2, t_3,\ (t_1 < t_2 < t_3)$ when $C(T)$ has extremal values. Because $0 < \Delta T_1 \equiv t_2 - t_1 < \Delta T_2 \equiv t_3 - t_2$, a deceleration at propagation velocity of MSTID is clarified. The GNSS station 1063 is used as the central station and the GPS satellite RRN17 is selected for the analysis.

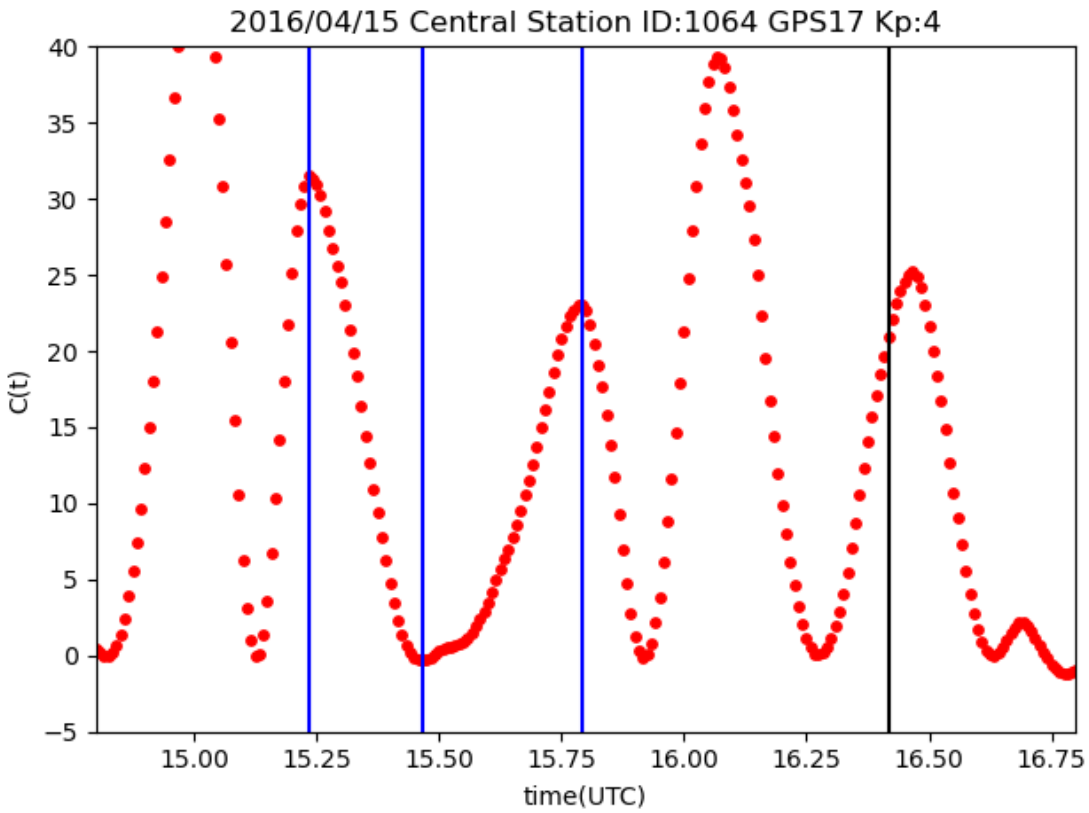

Figure S15. Correlation values before the 2016 Kumamoto earthquake (1064) on April 15, 2016

The vertical axis shows the correlation $C(T)$ and the horizontal one the time t (UTC). The black line indicates the exact time 16:25 (UTC) when the 2016 Kumamoto earthquake occurred. The blue lines indicate the times $t_1, t_2, t_3,\ (t_1 < t_2 < t_3)$ when $C(T)$ has extremal values. Because $0 < \Delta T_1 \equiv t_2 - t_1 < \Delta T_2 \equiv t_3 - t_2$, a deceleration at propagation velocity of MSTID is clarified. The GNSS station 1064 is used as the central station and the GPS satellite RRN17 is selected for the analysis.

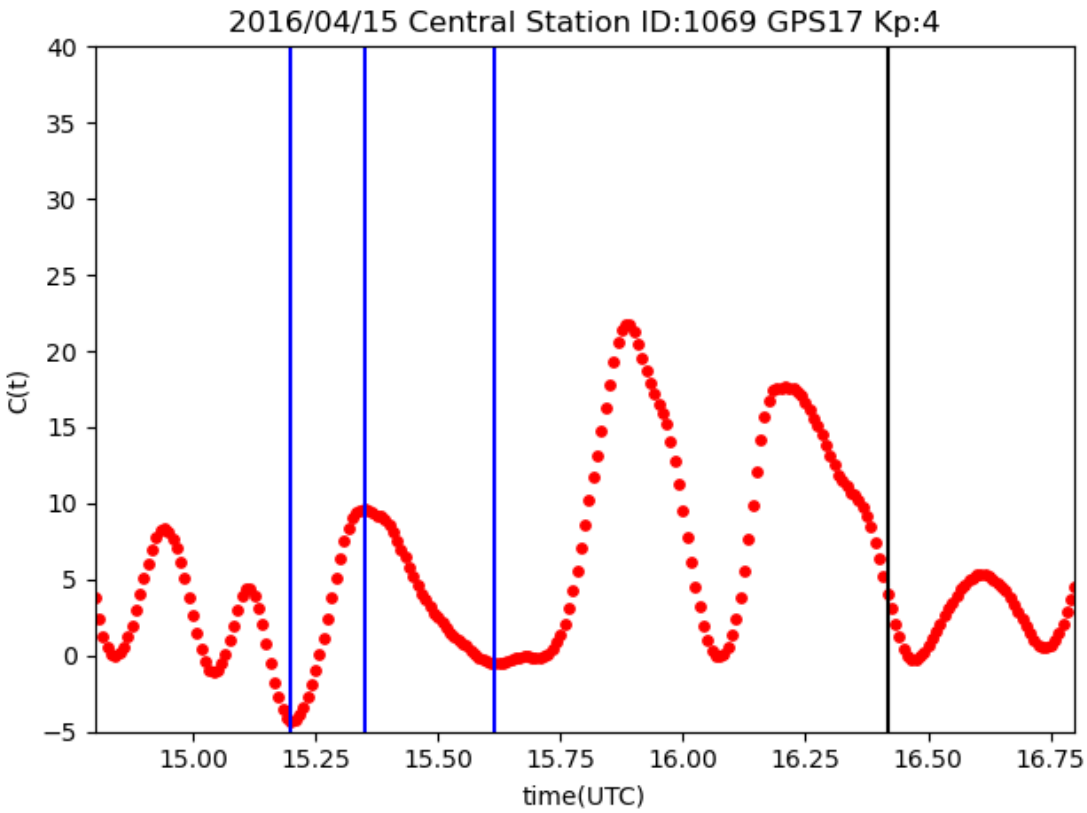

Figure S16. Correlation values before the 2016 Kumamoto earthquake (1069) on April 15, 2016

The vertical axis shows the correlation $C(T)$ and the horizontal one the time t (UTC). The black line indicates the exact time 16:25 (UTC) when the 2016 Kumamoto earthquake occurred. The blue lines indicate the times $t_1, t_2, t_3,\ (t_1 < t_2 < t_3)$ when $C(T)$ has extremal values. Because $0 < \Delta T_1 \equiv t_2 - t_1 < \Delta T_2 \equiv t_3 - t_2$, a deceleration at propagation velocity of MSTID is clarified. The GNSS station 1069 is used as the central station and the GPS satellite RRN17 is selected for the analysis.

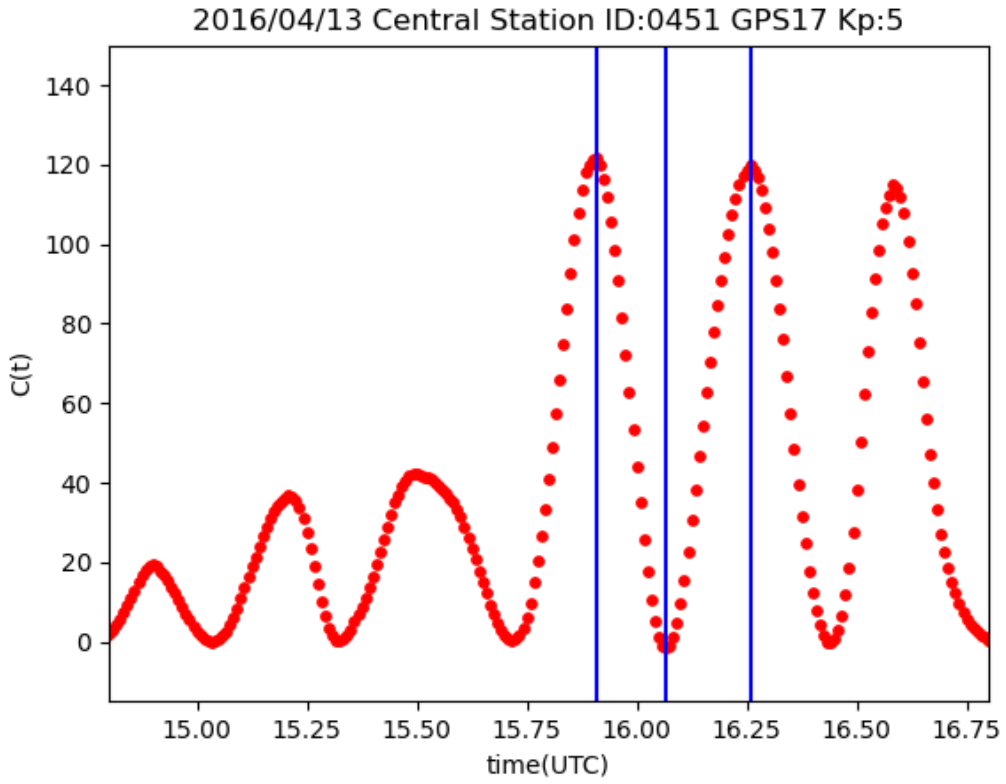

Figure S17. Correlation values (0451) on April 13, 2016

The vertical axis shows the correlation $C(T)$ and the horizontal one the time t (UTC). The blue lines indicate the times $t_1, t_2, t_3,\ (t_1 < t_2 < t_3)$ when $C(T)$ has extremal values. Because $\Delta T_1 \equiv t_2 - t_1 \simeq \Delta T_2 \equiv t_3 - t_2$, a deceleration of propagation velocity of MSTID is not detectable. We used the pair of the GNSS station 0451 as a central station and GPS satellite RRN17.

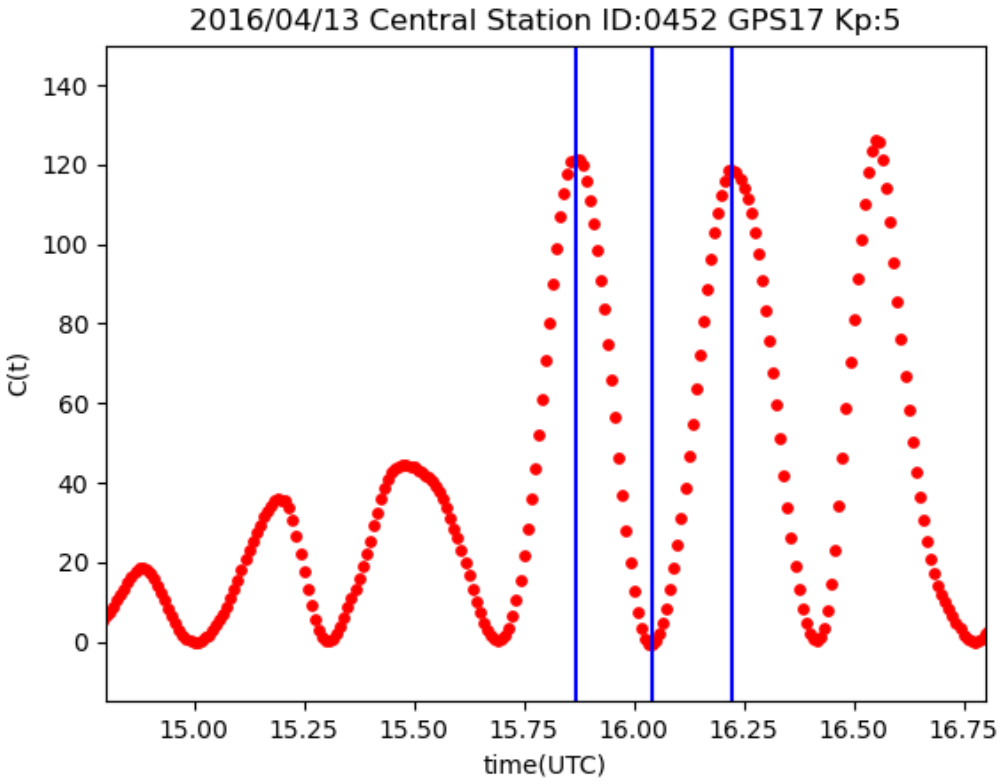

Figure S18. Correlation values (0452) on April 13, 2016

The vertical axis shows the correlation $C(T)$ and the horizontal one the time t (UTC). The blue lines indicate the times $t_1, t_2, t_3,\ (t_1 < t_2 < t_3)$ when $C(T)$ has extremal values. Because $\Delta T_1 \equiv t_2 - t_1 \simeq \Delta T_2 \equiv t_3 - t_2$, a deceleration of propagation velocity of MSTID is not detectable. We used the pair of the GNSS station 0452 as a central station and GPS satellite RRN17.

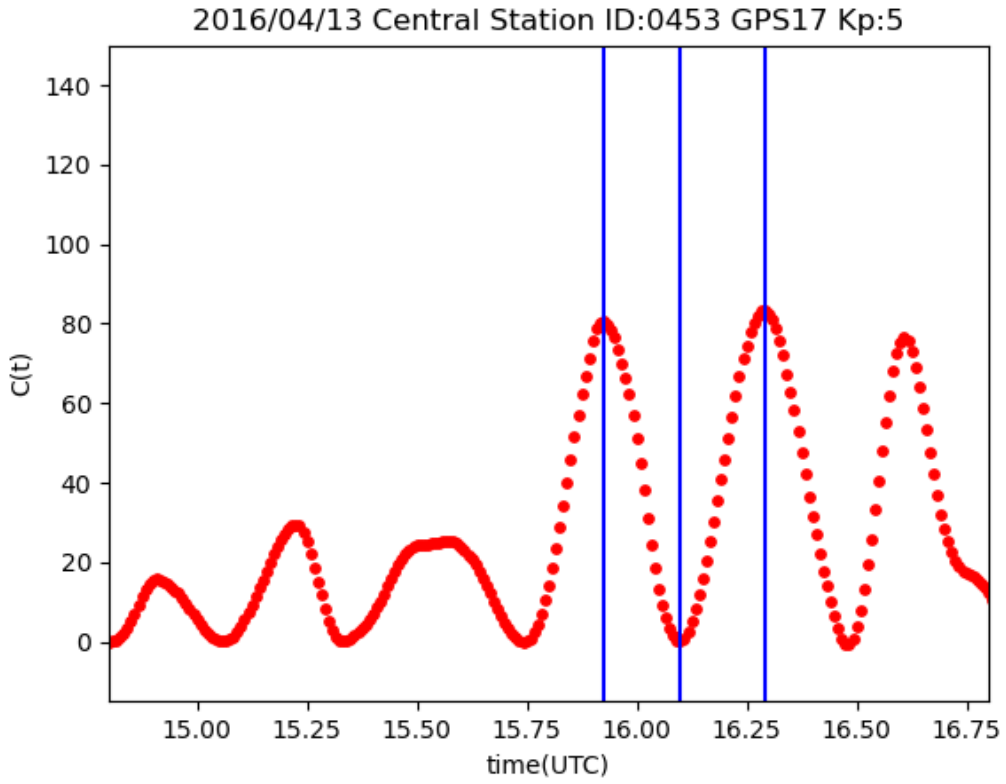

Figure S19. Correlation values (0453) on April 13, 2016

The vertical axis shows the correlation $C(T)$ and the horizontal one the time t (UTC). The blue lines indicate the times $t_1, t_2, t_3,\ (t_1 < t_2 < t_3)$ when $C(T)$ has extremal values. Because $\Delta T_1 \equiv t_2 - t_1 \simeq \Delta T_2 \equiv t_3 - t_2$, a deceleration of propagation velocity of MSTID is not detectable. We used the pair of the GNSS station 0453 as a central station and GPS satellite RRN17.

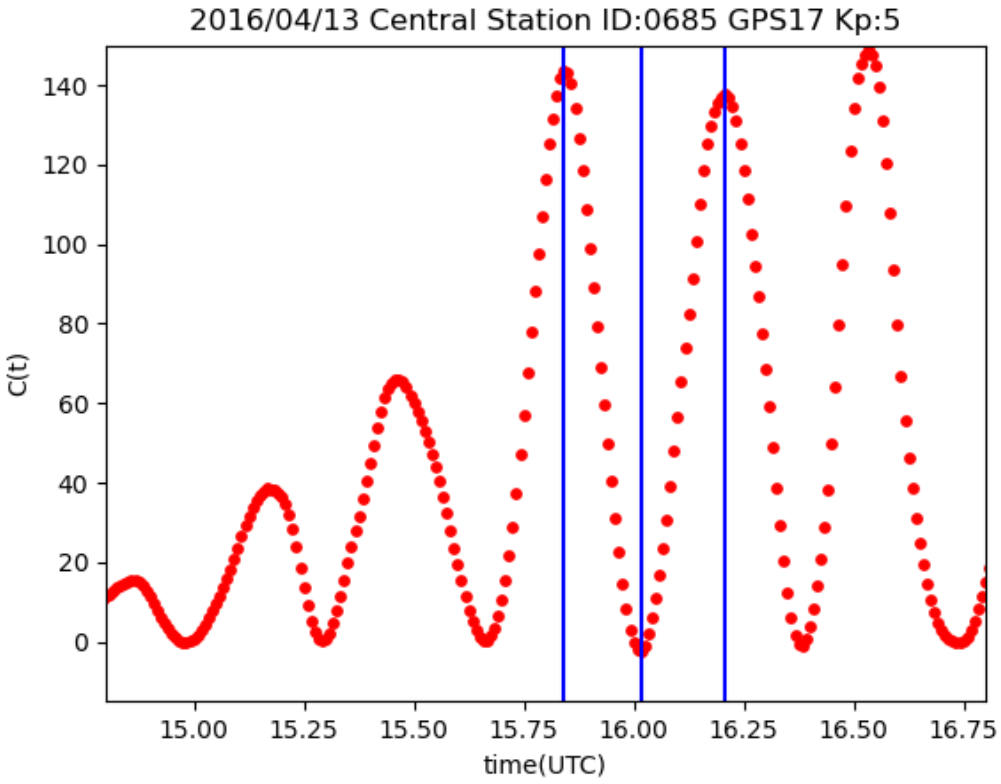

Figure S20. Correlation values (0685) on April 13, 2016

The vertical axis shows the correlation $C(T)$ and the horizontal one the time t (UTC). The blue lines indicate the times $t_1, t_2, t_3,\ (t_1 < t_2 < t_3)$ when $C(T)$ has extremal values. Because $\Delta T_1 \equiv t_2 - t_1 \simeq \Delta T_2 \equiv t_3 - t_2$, a deceleration of propagation velocity of MSTID is not detectable. We used the pair of the GNSS station 0685 as a central station and GPS satellite RRN17.

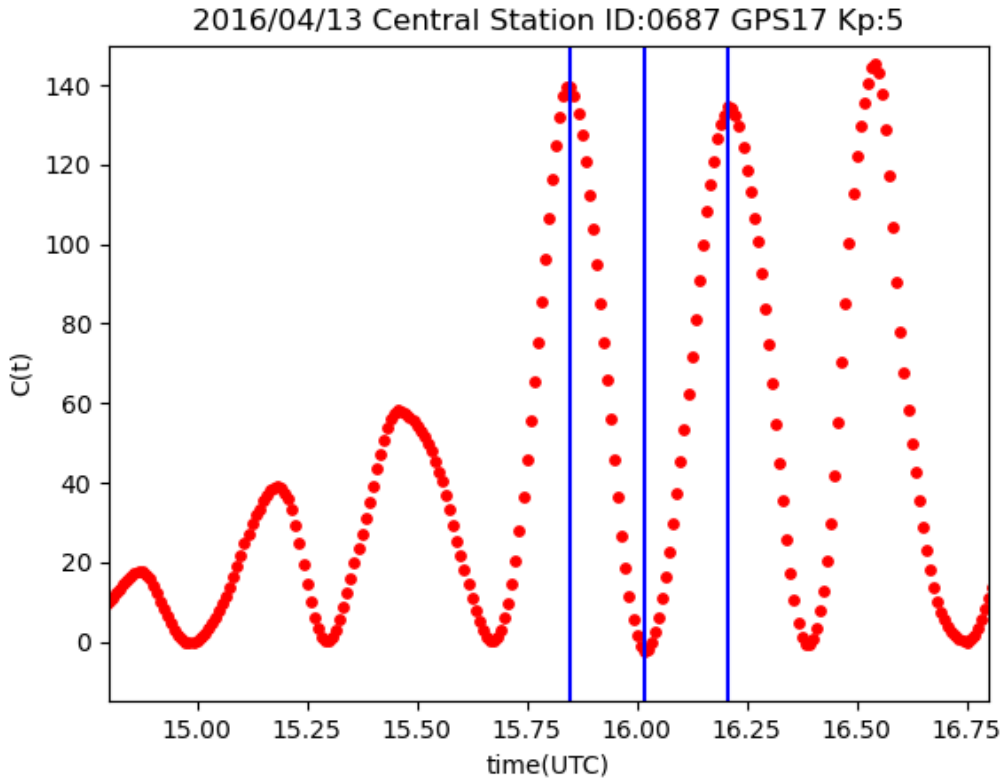

Figure S21. Correlation values (0687) on April 13, 2016

The vertical axis shows the correlation $C(T)$ and the horizontal one the time t (UTC). The blue lines indicate the times $t_1, t_2, t_3,\ (t_1 < t_2 < t_3)$ when $C(T)$ has extremal values. Because $\Delta T_1 \equiv t_2 - t_1 \simeq \Delta T_2 \equiv t_3 - t_2$, a deceleration of propagation velocity of MSTID is not detectable. We used the pair of the GNSS station 0687 as a central station and GPS satellite RRN17.

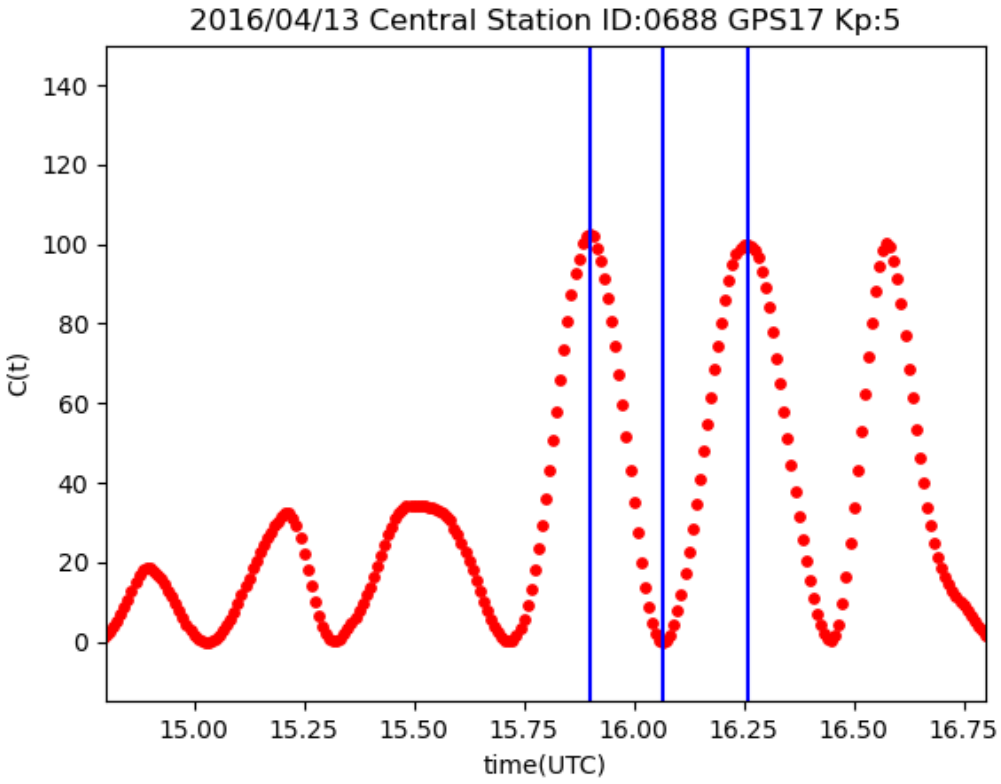

Figure S22. Correlation values (0688) on April 13, 2016

The vertical axis shows the correlation $C(T)$ and the horizontal one the time t (UTC). The blue lines indicate the times $t_1, t_2, t_3,\ (t_1 < t_2 < t_3)$ when $C(T)$ has extremal values. Because $\Delta T_1 \equiv t_2 - t_1 \simeq \Delta T_2 \equiv t_3 - t_2$, a deceleration of propagation velocity of MSTID is not detectable. We used the pair of the GNSS station 0688 as a central station and GPS satellite RRN17.

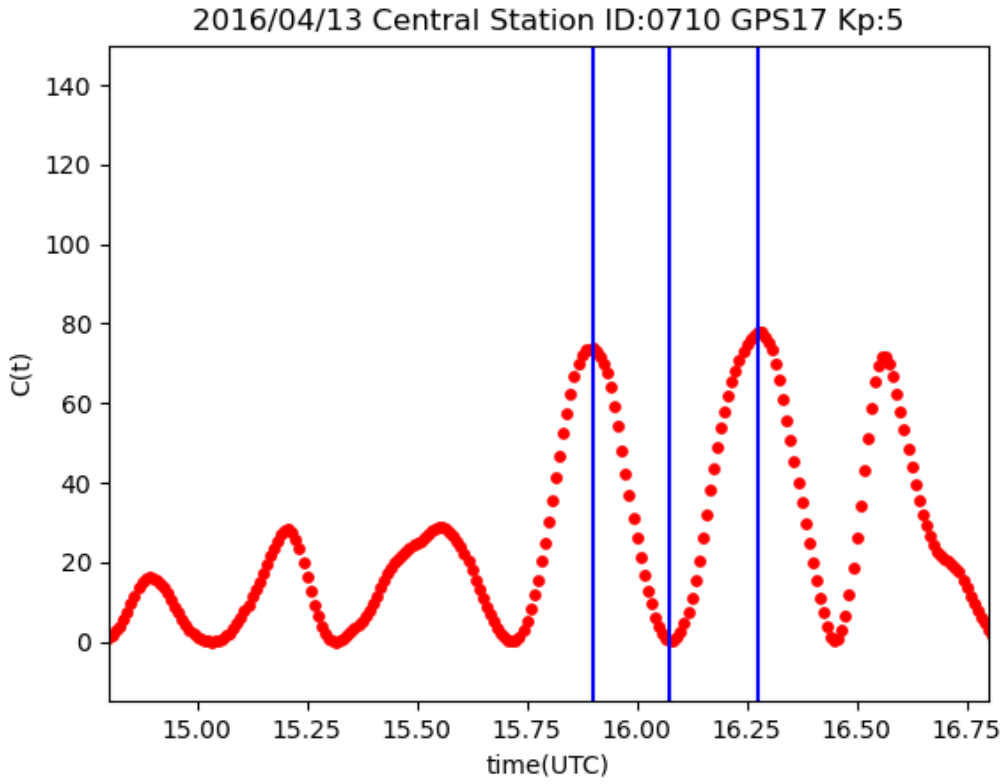

Figure S23. Correlation values (0710) on April 13, 2016

The vertical axis shows the correlation $C(T)$ and the horizontal one the time t (UTC). The blue lines indicate the times $t_1, t_2, t_3,\ (t_1 < t_2 < t_3)$ when $C(T)$ has extremal values. Because $\Delta T_1 \equiv t_2 - t_1 \simeq \Delta T_2 \equiv t_3 - t_2$, a deceleration of propagation velocity of MSTID is not detectable. We used the pair of the GNSS station 0710 as a central station and GPS satellite RRN17.

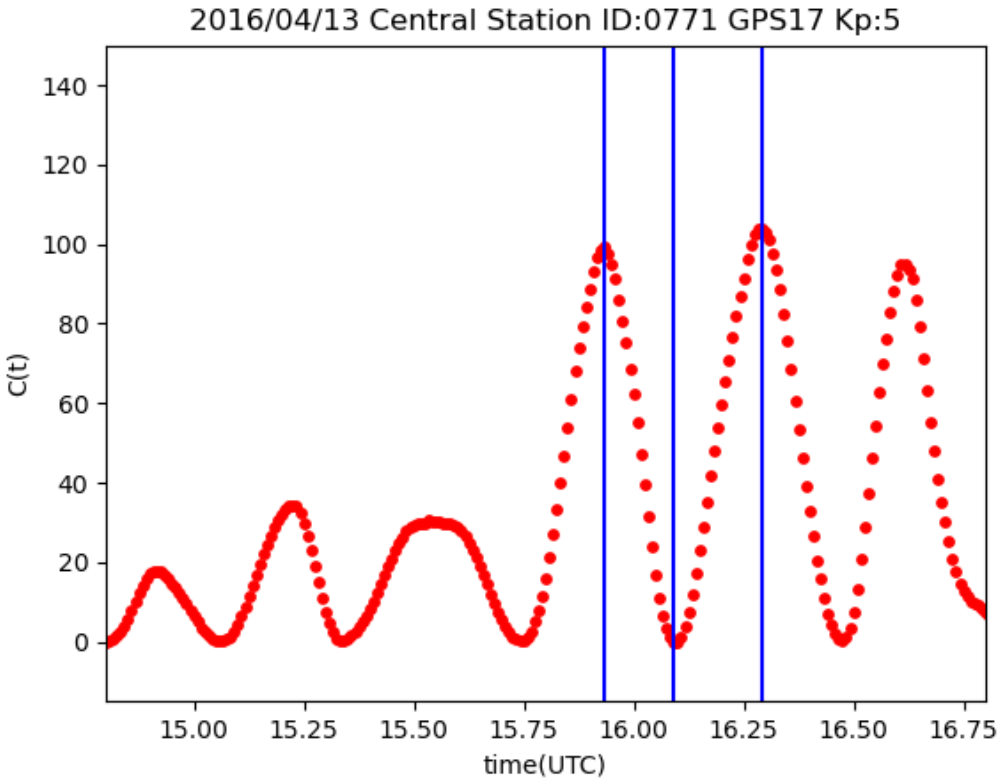

Figure S24. Correlation values (0771) on April 13, 2016

The vertical axis shows the correlation $C(T)$ and the horizontal one the time t (UTC). The blue lines indicate the times $t_1, t_2, t_3,\ (t_1 < t_2 < t_3)$ when $C(T)$ has extremal values. Because $\Delta T_1 \equiv t_2 - t_1 \simeq \Delta T_2 \equiv t_3 - t_2$, a deceleration of propagation velocity of MSTID is not detectable. We used the pair of the GNSS station 0771 as a central station and GPS satellite RRN17.

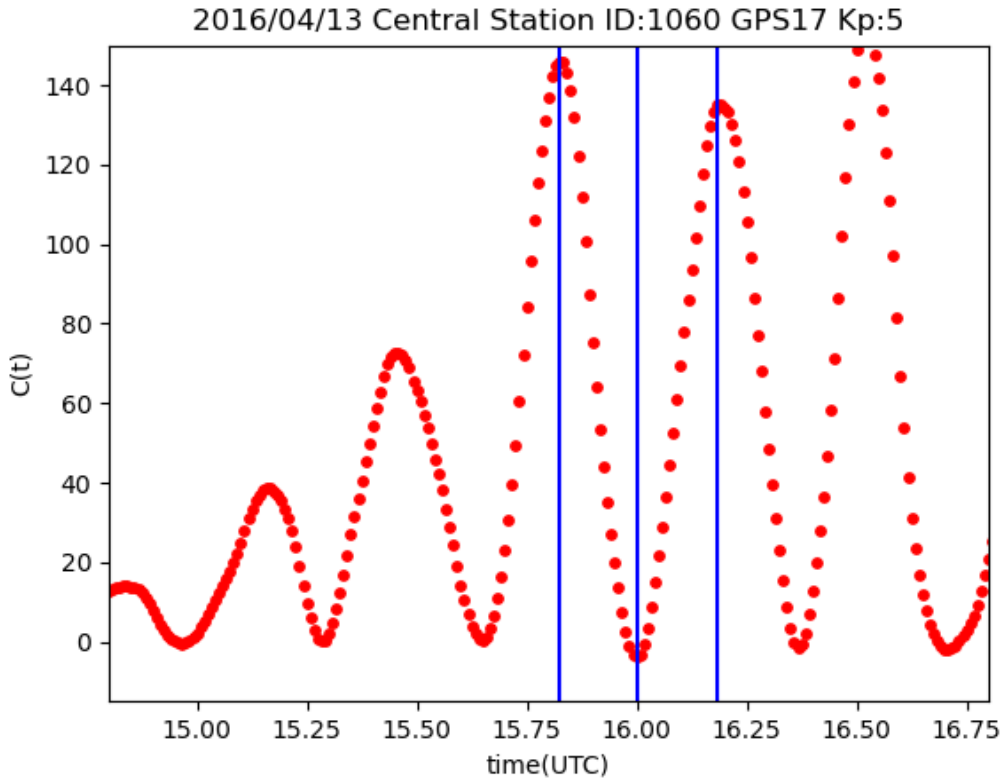

Figure S25. Correlation values (1060) on April 13, 2016

The vertical axis shows the correlation $C(T)$ and the horizontal one the time t (UTC). The blue lines indicate the times $t_1, t_2, t_3,\ (t_1 < t_2 < t_3)$ when $C(T)$ has extremal values. Because $\Delta T_1 \equiv t_2 - t_1 \simeq \Delta T_2 \equiv t_3 - t_2$, a deceleration of propagation velocity of MSTID is not detectable. We used the pair of the GNSS station 1060 as a central station and GPS satellite RRN17.

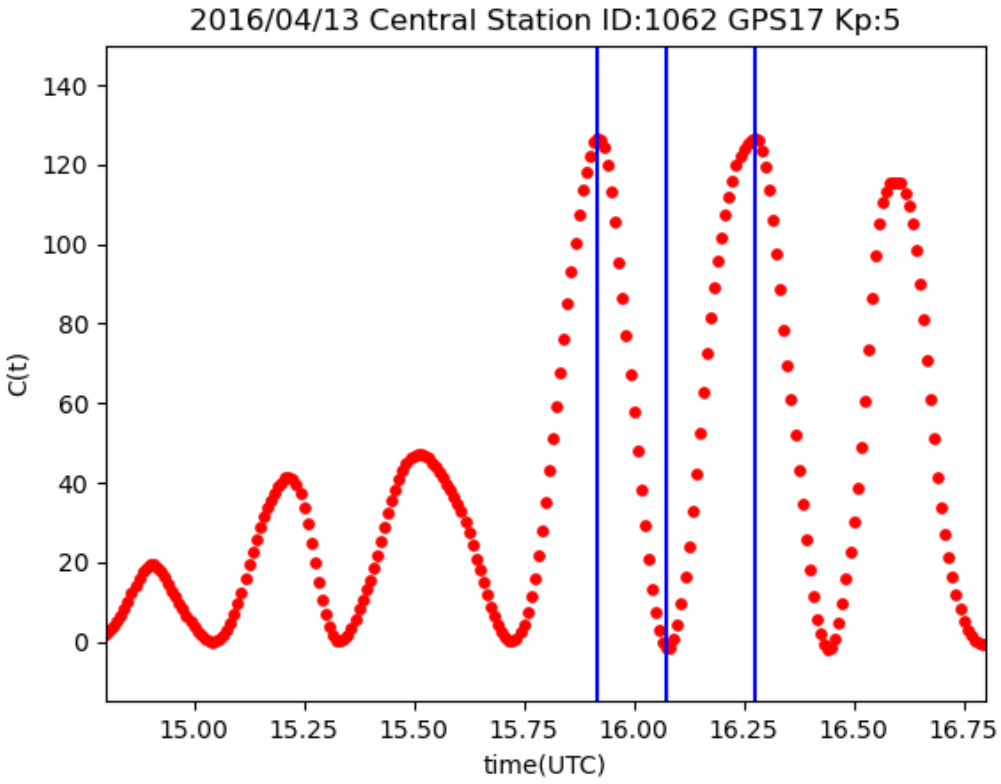

Figure S26. Correlation values (1062) on April 13, 2016

The vertical axis shows the correlation $C(T)$ and the horizontal one the time t (UTC). The blue lines indicate the times $t_1, t_2, t_3,\ (t_1 < t_2 < t_3)$ when $C(T)$ has extremal values. Because $\Delta T_1 \equiv t_2 - t_1 \simeq \Delta T_2 \equiv t_3 - t_2$, a deceleration of propagation velocity of MSTID is not detectable. We used the pair of the GNSS station 1062 as a central station and GPS satellite RRN17.

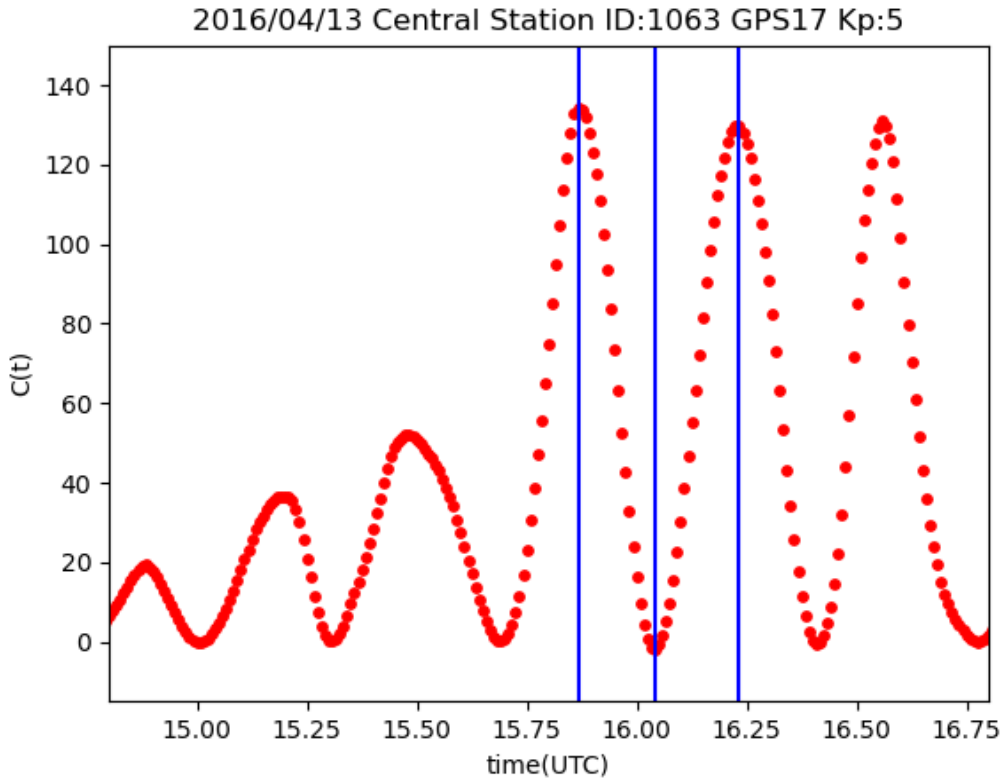

Figure S27. Correlation values (1063) on April 13, 2016

The vertical axis shows the correlation $C(T)$ and the horizontal one the time t (UTC). The blue lines indicate the times $t_1, t_2, t_3,\ (t_1 < t_2 < t_3)$ when $C(T)$ has extremal values. Because $\Delta T_1 \equiv t_2 - t_1 \simeq \Delta T_2 \equiv t_3 - t_2$, a deceleration of propagation velocity of MSTID is not detectable. We used the pair of the GNSS station 1063 as a central station and GPS satellite RRN17.

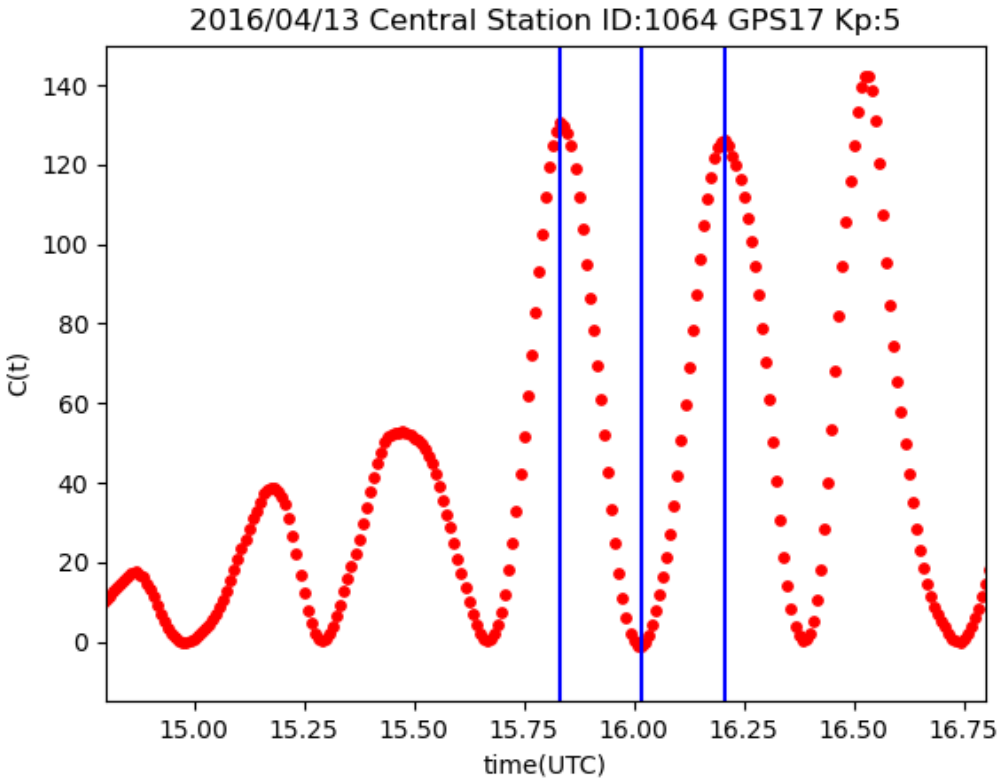

Figure S28. Correlation values (1064) on April 13, 2016

The vertical axis shows the correlation $C(T)$ and the horizontal one the time t (UTC). The blue lines indicate the times $t_1, t_2, t_3,\ (t_1 < t_2 < t_3)$ when $C(T)$ has extremal values. Because $\Delta T_1 \equiv t_2 - t_1 \simeq \Delta T_2 \equiv t_3 - t_2$, a deceleration of propagation velocity of MSTID is not detectable. We used the pair of the GNSS station 1064 as a central station and GPS satellite RRN17.

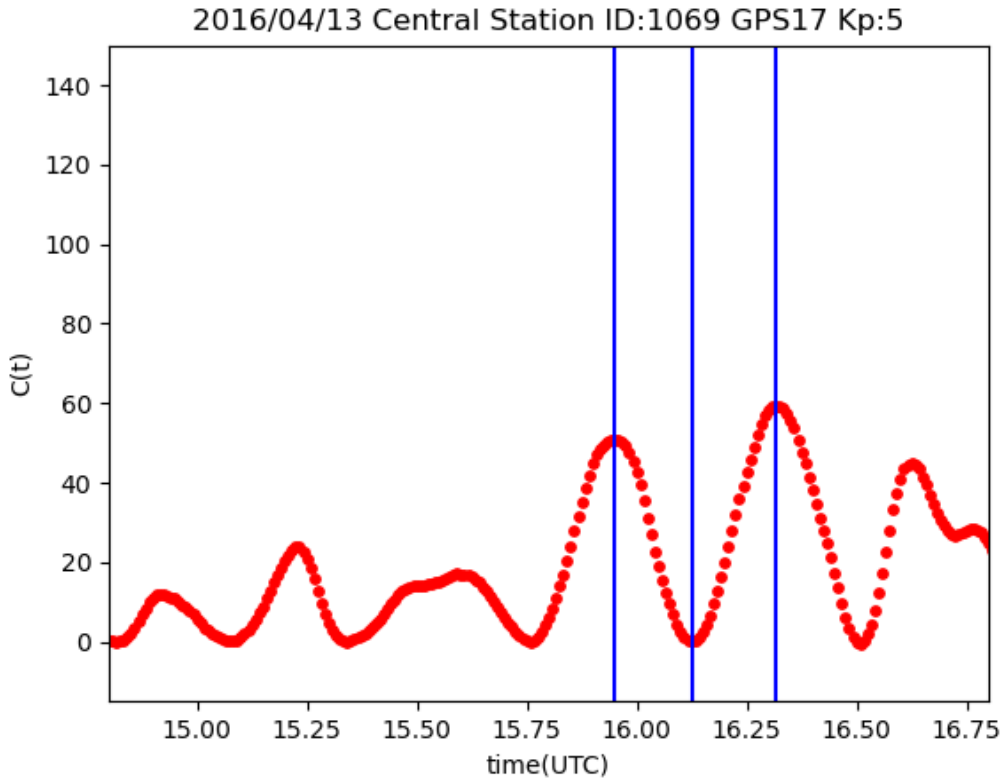

Figure S29. Correlation values (1069) on April 13, 2016

The vertical axis shows the correlation $C(T)$ and the horizontal one the time t (UTC). The blue lines indicate the times $t_1, t_2, t_3,\ (t_1 < t_2 < t_3)$ when $C(T)$ has extremal values. Because $\Delta T_1 \equiv t_2 - t_1 \simeq \Delta T_2 \equiv t_3 - t_2$, a deceleration of propagation velocity of MSTID is not detectable. We used the pair of the GNSS station 1069 as a central station and GPS satellite RRN17.

Table S1. Half Periods of MSTIDs on April 13, 2016 Estimated by CRA

Station	ΔT_1 (hour)	ΔT_2 (hour)	Ratio $\gamma \left(\equiv \frac{\Delta T_1}{\Delta T_2}\right)$	t_1 (UTC)	t_2 (UTC)	t_3 (UTC)
0087	0.167	0.183	0.909	15.883	16.050	16.233
0089	0.175	0.192	0.913	15.875	16.050	16.242
0451	0.158	0.192	0.826	15.908	16.067	16.258
0452	0.175	0.183	0.955	15.867	16.042	16.225
0453	0.175	0.192	0.913	15.925	16.100	16.292
0685	0.175	0.192	0.913	15.842	16.017	16.208
0687	0.167	0.192	0.870	15.850	16.017	16.208
0688	0.167	0.192	0.870	15.900	16.067	16.258
0710	0.175	0.200	0.875	15.900	16.075	16.275
0771	0.158	0.200	0.792	15.933	16.092	16.292
1060	0.175	0.183	0.955	15.825	16.000	16.183
1062	0.158	0.200	0.792	15.917	16.075	16.275
1063	0.175	0.192	0.913	15.867	16.042	16.233
1064	0.183	0.192	0.957	15.833	16.017	16.208
1069	0.175	0.192	0.913	15.950	16.125	16.317